Metabolic Engineering Communications 5 (2017) 26–33

Contents lists available at ScienceDirect

Metabolic Engineering Communications

journal homepage: www.elsevier.com/locate/mec

Flux balance analysis indicates that methane is the lowest cost feedstock for microbial cell factories

Austin D. Comer[a], Matthew R. Long[a], Jennifer L. Reed[a], Brian F. Pfleger[a,b,*]

[a] Department of Chemical and Biological Engineering, University of Wisconsin-Madison, Madison, WI 53706, United States
[b] Microbiology Doctoral Training Program, University of Wisconsin-Madison, Madison, WI 53706, United States

ABSTRACT

The low cost of natural gas has driven significant interest in using C_1 carbon sources (e.g. methane, methanol, CO, syngas) as feedstocks for producing liquid transportation fuels and commodity chemicals. Given the large contribution of sugar and lignocellulosic feedstocks to biorefinery operating costs, natural gas and other C_1 sources may provide an economic advantage. To assess the relative costs of these feedstocks, we performed flux balance analysis on genome-scale metabolic models to calculate the maximum theoretical yields of chemical products from methane, methanol, acetate, and glucose. Yield calculations were performed for every metabolite (as a proxy for desired products) in the genome-scale metabolic models of three organisms: *Escherichia coli* (bacterium), *Saccharomyces cerevisiae* (yeast), and *Synechococcus* sp. PCC 7002 (cyanobacterium). The calculated theoretical yields and current feedstock prices provided inputs to create comparative feedstock cost surfaces. Our analysis shows that, at current market prices, methane feedstock costs are consistently lower than glucose when used as a carbon and energy source for microbial chemical production. Conversely, methanol is costlier than glucose under almost all price scenarios. Acetate feedstock costs could be less than glucose given efficient acetate production from low-cost syngas using nascent biological gas to liquids (BIO-GTL) technologies. Our analysis suggests that research should focus on overcoming the technical challenges of methane assimilation and/or yield of acetate via BIO-GTL to take advantage of low-cost natural gas rather than using methanol as a feedstock.

1. Introduction

Abundant, low cost C_1 compounds such as methane, methanol, and carbon monoxide have garnered attention as potentially inexpensive sources of carbon and energy in biocatalytic processes for producing commodity chemicals (Conrado and Gonzalez, 2014; Haynes and Gonzalez, 2014; Whitaker et al., 2015). Over the last decade, natural gas supply has reached all-time highs with costs consistently lower than petroleum. Despite these economic advantages, large volumes of natural gas are flared at wellheads daily to reduce greenhouse gas emissions or directly leaked, both intentionally and unintentionally, to the environment during production (Howarth et al., 2011; Salmon and Logan, 2013). Nighttime satellite images of these areas show light intensities equivalent to major US cities and illustrate the enormous potential that is wasted. Alternative uses, such as pipelining to refineries, catalytic conversion to syngas or methanol, or combustion for electricity and heat have not been deployed due to costs, wide geographic distribution, and/or poor proximity to end-users. Given that feedstocks are the major operating cost of producing biomanufactured chemicals (Klein-Marcuschamer et al., 2011), the choice of carbon source can have a significant impact on profitability. Given the potential process advantages, the economic potential of C_1 feedstocks for biomanufacturing of commodity chemicals warrants evaluation.

Cost is not the only criteria when considering methane, as gas-phase feedstocks suffer from a few bioprocess drawbacks. First, uptake of gas-phase feedstocks can be mass-transfer limited and significantly slower than uptake of traditional aqueous feedstocks, such as sugars and organic acids, depending on bioreactor conditions (Conrado and Gonzalez, 2014). Second, methane utilization by methylotrophs requires an electron acceptor – most frequently oxygen – which raises safety concerns over potentially explosive mixtures of feedstock gases (Whitaker et al., 2015). Third, the conversion of methane to methanol, catalyzed by methane monooxgynease, is a slow step that limits overall productivity. For these reasons, we were curious if alternative derivatives of C_1 compounds, methanol and acetate, would have economic advantages over glucose. Methanol, produced by steam reformation to syngas and catalytic conversion to methanol, is the first intermediate in methane assimilation. Acetate can be produced from natural gas by

* Corresponding author at: Department of Chemical and Biological Engineering, University of Wisconsin-Madison, Madison, WI 53706, United States.
E-mail address: pfleger@engr.wisc.edu (B.F. Pfleger).

http://dx.doi.org/10.1016/j.meteno.2017.07.002
Received 31 March 2017; Received in revised form 23 June 2017; Accepted 5 July 2017
Available online 10 July 2017

combining catalytic water-gas shift with anaerobic fermentation of the resulting syngas by acetogens. These so-called biological gas-to-liquid (Bio-GTL) processes have been recently demonstrated for producing lipids and biodiesel (Hu et al., 2016). This low-cost process makes acetate an interesting potential feedstock to replace glucose in biocatalytic processes. Feeding aqueous methanol or acetate would circumvent many of the technical hurdles in a bioreactor while potentially leveraging the low-cost and abundant supply of C_1 feedstocks.

The last factor in selecting a feedstock is the relative amount needed to generate a given amount of product. Sugars are the dominant feedstock for bioconversions because metabolism efficiently extracts energy and electrons for use in synthesizing chemical products. Assimilation of C1 compounds is not as energy efficient given higher energy and reducing power costs. There are several pathways for assimilating methane and methanol; each differs in energetic yield, connections to central metabolism, and kinetics. Methane and methanol assimilation both occur through the assimilation of formaldehyde. The first step in methane catabolism is oxidation to methanol by a methane monooxygenase (Hwang et al., 2014). Methanol is further oxidized to formaldehyde by an alcohol oxidase or methanol dehydrogenase (Müller et al., 2015; Whitaker et al., 2015). Formaldehyde is then assimilated through one of three pathways: the ribulose monophosphate (RuMP) pathway, the dihydroxyacetone (DHA) pathway, or the serine pathway (Fig. 1) (Yurimoto et al., 2005). The DHA — found only in fungi — and RuMP — common in gamma-proteobacteria and only found in bacteria and archea — pathways both use a five carbon sugar as a substrate to assimilate formaldehyde and produce a six carbon sugar (Hwang et al., 2014; Müller et al., 2015; Whitaker et al., 2015; Yurimoto et al., 2005). Every three turnovers of these cycles produces a single dihydroxyacetone phosphate. In contrast, the serine pathway — common in alpha-proteobacteria — assimilates formaldehyde through reaction with glycine to create serine (Hwang et al., 2014; Yurimoto et al., 2005). Every two turnovers of this cycle assimilates two formaldehydes and one carbon dioxide to produce a 2-phosphoglycerate (the base cycle can be augmented with other reactions to produce acetyl-CoA and TCA cycle intermediates with additional cycles and assimilation of CO_2). To obtain energy, formaldehyde is oxidized to carbon dioxide to generate reducing equivalents that can be converted to ATP via the electron transport chain and ATP synthase (Yurimoto et al., 2005). Overall, the RuMP pathway is considered the most efficient pathway in terms of energetic yield and is the preferred C_1 assimilation pathway in studies of C_1 catabolism as a feedstock (Müller et al., 2015). Beyond the formaldehyde assimilating pathways, there is a small class of C_1 catabolizing, non-photosynthetic bacteria that use the Calvin-Benson-Bassham (CBB) cycle to assimilate carbon dioxide by oxidation of C_1 carbon sources to produce the energy needed to run the CBB (Hwang et al., 2014). This does not appear to be an efficient pathway and is not biologically common, so we did not include it in our analysis. In addition, Bogorad et al. (2014, 2013) created a synthetic methanol condensation cycle (MCC) for the efficient assimilation of methanol by using a combination of the RuMP cycle and synthetic non-oxidative glycolysis in *Escherichia coli*. We tested this pathway for improved yield as part of a set of analysis looking at the impact of including carbon efficient assimilation pathways and show little difference on predicted product yields in *E. coli*.

Acetate is typically assimilated into central metabolism as acetyl-CoA. Acetate is a common by-product during rapid growth in bacteria and re-assimilates during stationary phase at the cost of one ATP. For this reason, most organisms, including those studied here, have pathways for assimilating acetate. In *E. coli*, and many other microorganisms, acetate assimilation proceeds through acetyl-phosphate (catalyzed by ackA/pta). In other organisms, such as the cyanobacterium *Synechococcus* sp. strain PCC 7002 studied here, acetate assimilation proceeds through a transient acyl-AMP intermediate as part of an acyl-CoA ligase mechanism (Begemann et al., 2013). Other pathways for acetate assimilation involve CoA transfer from other metabolites (e.g. propionyl-CoA, succinyl-CoA).

To assess the tradeoffs between feedstock cost and product yield, we have performed an economic analysis using maximum theoretical yields calculated by flux balance analysis of genome-scale metabolic models. We performed the analysis on models of three organisms, the bacterium *E. coli*, the yeast *Saccharomyces cerevisiae*, and the cyanobacterium *Synechococcus* sp. strain PCC 7002, augmented with all three common methane assimilation pathways (serine, RUMP, DHA). For each model, we calculated the theoretical yield for every metabolite in each model from each feedstock – glucose, methane, methanol, and acetate as well as xylose and glycerol for *E. coli* only. We use the calculated theoretical yields and current feedstock prices to create surfaces of feedstock costs. Our analysis shows that despite the lower stoichiometric yield from methane, methane feedstock costs are consistently lower than glucose when used as carbon and energy sources to make products. Conversely, methanol is equal to or costlier than glucose. Acetate is much more difficult to give an accurate estimate of comparable feedstock cost with glucose given current technological change and price variation. Our analysis suggests that methane is the most promising C_1 feedstock, assuming it is possible to overcome any technical hurdles associated with its use as a feedstock.

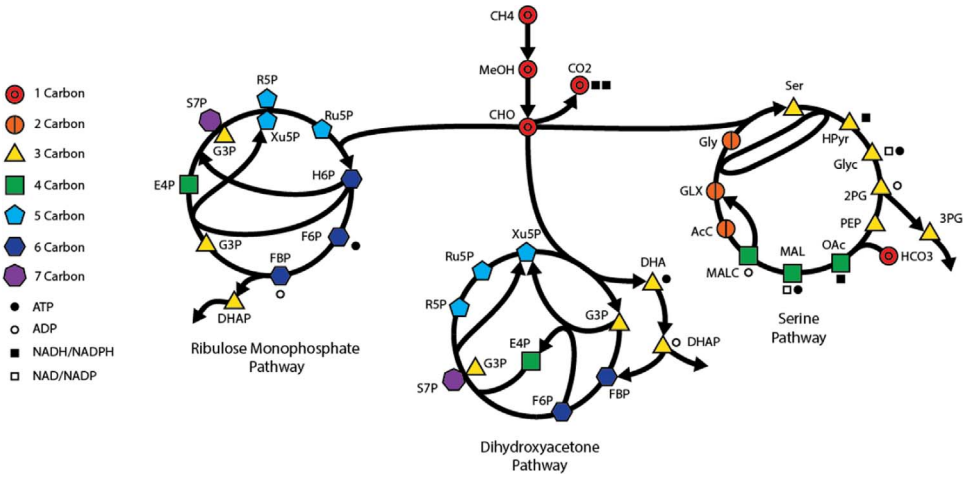

Fig. 1. Formaldehyde assimilation pathways. The ribulose mono-phosphate (RuMP) pathway is a bacterial formaldehyde assimilation pathway that uses ribulose-5-phosphate as a substrate for formaldehyde assimilation. The dihydroxyacetone (DHA) pathway is a fungal formaldehyde assimilation pathway that uses xylulose-5-phosphate as a substrate for formaldehyde assimilation. The serine pathway is a bacterial pathway that uses glycine to assimilate formaldehyde. The serine pathway also assimilates one carbon dioxide for every two formaldehydes assimilated. All three pathways produce glycolytic intermediates. The abbreviations are defined as follows: CH4 – methane, MeOH – methanol, CHO – formaldehyde, CO2 – carbon dioxide, H6P – hexulose 6-phosphate, F6P – fructose 6-phosphate, FBP – fructose 1,6 bisphosphate, DHAP – dihydroxyacetone phosphate, G3P – glyceraldehyde 3-phosphate, E4P – eyrthrose 4-phosphate, S7P – septulose 7-phosphate, R5P – ribose 5-phosphate, Xu5P – xylulose 5-phosphate, Ru5P – ribulose 5-phosphate, DHA – dihydroxyacetone, Ser – serine, HPyr – hydroxypyruvate, Glyc – glycerate, 2PG – 2-phosphoglycerate, 3PG –3-phosphoglycerate, PEP – phosphoenolpyruvate, HCO3 – bicarbonate, OAc – oxaloacetate, MAL – malate, MALC – malyl-CoA, AcC – acetyl-CoA, GLX – glyoxylate, GLY – glycine.

2. Methods

2.1. Genome-scale metabolic modeling

Established genome-scale metabolic models of *E. coli* (iJO1366) (Orth et al., 2011), *S. cerevisiae* (iMM904) (Mo et al., 2009), and *Synechococcus* sp. strain PCC 7002 (iSYP708) (Vu et al., 2013) were used to calculate theoretical yields. Each model was augmented with reactions necessary for C_1 metabolism, including methane/methanol exchange, methane/methanol transport, methane/methanol oxidation, the RuMP pathway, the DHA pathway, the serine pathway, and formaldehyde oxidation to carbon dioxide. Acetate assimilation pathways were already present in each model. For PCC 7002, which lacks a glyoxylate shunt, acetate is assimilated as acetyl-CoA that is respired through an alternate TCA cycle present in cyanobacteria. The resulting reducing equivalents are used to create ATP through the electron transport chain and to fix CO_2 via the Calvin cycle to fix. A complete table of the modeled media and uptake constraints are in Supplementary Tables 1–3. All reactions that were added to the base models are listed in Supplementary Tables 4–6. Reactions for heterologous pathways or carbon efficient pathways were not included in the augmented model during yield ratio calculations. These were only included individually for additional analyses. Please note genome scale metabolic models are only capable of simulating the biological features that are encoded within the model. Our chosen *S. cerevisiae* and S. PCC 7002 models are less developed than the widely accepted *E. coli* model and therefore may not capture all biological features.

Flux balance analysis (FBA) was used to calculate the maximum theoretical yield of specific metabolites under carbon-limited conditions for each augmented model (Orth et al., 2010; Papoutsakis, 2000). The yields were calculated for every metabolite within a model. The formulation is shown in (1) where I is the set of all metabolites and J is the set of all reactions. I^{target} is the target metabolite for the current iteration. $S_{i,j}$ is the stoichiometric matrix, v_j is the flux vector, and p_i is a metabolite accumulation rate vector. p_i is constrained to zero for all metabolites besides the metabolite whose yield is being maximized (I^{target}). Biomass generation was either unconstrained or forced to be greater than or equal to 10% of the maximum biomass exchange flux for each substrate. Calculations were performed for the carbon sources: methane, methanol, glucose, acetate, glycerol (*E. coli* only), and xylose (*E. coli* only).

$$\max_{v,p} \sum_{i \in I^{target}} p_i \tag{1a}$$

$$\sum_{j \in J} S_{i,j} \bullet v_j = p_i \quad \forall \quad i \in I \tag{1b}$$

$$p_i = 0 \quad \forall \quad i \notin I^{target} \tag{1c}$$

$$\alpha_j \leq v_j \leq \beta_j \quad \forall \; j \in J \tag{1d}$$

All models were solved with the assumption that cells could uptake unlimited amounts of O_2 (aerobic conditions) and other inorganic nutrients (metals, phosphate, ammonium, protons, etc.) required for growth and/or to balance metabolism. Carbon uptake was restricted to a maximum of 10 mmol/gDW/h of each substrate. The *E. coli* model included a term for maintenance energy, which was set to 3.15 mmol/gDW/h as determined by Orth *et al.* (Orth et al., 2011). In the yeast model, we added all augmented reactions to the cytoplasm compartment. The cyanobacterial model (iSYP708) contains a light uptake constraint of zero forcing cells to uptake a single carbon/energy source. These simulations were performed to evaluate the impact of different carbon sources on improving chemical production through a diurnal light/dark cycle (McEwen et al., 2013).

2.2. Economic analysis

To evaluate each feedstock, we calculated the relative feedstock costs for producing one mole of each metabolite in the metabolic models. Dividing the molar price of each feedstock by the theoretical yield of that feedstock yields the individual feedstock cost. Here, we used Eq. (2) to calculate an average relative feedstock cost (RC) between glucose and an alternate carbon source. In Eq. (2), YR represents ratio of theoretical yields (molar yield on the alternative carbon source divided by molar yield on glucose), P_a is the molar price of the alternate carbon source, and P_g is the molar price of glucose. YR is estimated by a linear regression through the origin between the molar yields of each metabolite when produced using glucose and the alternative carbon source. The sensitivity of the relative feedstock cost was calculated by varying feedstock prices and creating a surface for visualization.

$$RC = \frac{P_a}{P_g} * \frac{1}{YR} \tag{2}$$

3. Results

3.1. Molar theoretical yields

In order to assess the relative value of feedstocks for producing chemicals, we performed flux balance analysis of three genome-scale metabolic models augmented with reactions required for assimilating C_1 substrates. We compared the maximum theoretical yield of each metabolite from alternative carbon sources – methane, methanol, and acetate – to the corresponding yield on glucose (Fig. 2**a–c**). In each case, there was a strong correlation with a high R_0^2 value for a linear regression through the origin. In subsequent analyses, we used the slope of the regression to represent the ratio of theoretical yield of chemicals from each feedstock and organism. Among the feedstocks, glucose gave the highest theoretical yield followed by acetate, methanol, and methane, consistent with the number of carbons in each feedstock. Interestingly, methane, which is more reduced than methanol, has lower yields. This can be explained by the high cost of activating the C-H bond in methane, which requires a reducing equivalent. This investment is not recovered in the net exothermic reaction of methane conversion to methanol. When normalized by carbon number in the feedstock (Fig. 2**d**) the curves collapse and show interesting differences in slope depending on the organism. For *E. coli*, these curves collapse with $YR_{methanol} > YR_{methane} \sim YR_{glucose} > YR_{acetate}$. For *S. cerevisiae*, these curves collapse with $YR_{methanol} \sim YR_{glucose} > YR_{acetate} \sim YR_{methane}$. For *S.* PCC7002, these curves collapse with $YR_{methanol} \sim YR_{methane} > YR_{acetate} > YR_{glucose}$. Supplemental Table 7 summarizes the ratios of theoretical yield.

Both methanol and glycerol had higher carbon yields than glucose for *E. coli* while only methanol had a higher carbon yield for *S. cerevisiae* (Fig. 2**d and** Supplemental Table 7). For *S.* PCC7002: methane, methanol, and acetate all had higher carbon yields than glucose, which suggests *S.* PCC7002 may not utilize glucose as efficiently. The maximum P/O ratios for each metabolic model was calculated (Supplemental Table 8). The *E. coli* model had a higher P/O value (1.375) than the *S. cerevisiae* model (1.125), which could explain why maximum yields for some compounds were higher in *E. coli* than *S. cerevisiae*. *S.* PCC7002 had the highest P/O ratio at 2.5; however, this is based on genome annotations and should be confirmed experimentally.

3.2. Impact of specific pathways

With unconstrained growth, most solutions resulted in no biomass generation, while some required growth to generate the product. We repeated our analysis to require biomass production of at least 10% of the maximum biomass generation rate (for a given feedstock) to see if consistent relative theoretical yields were maintained. As seen in

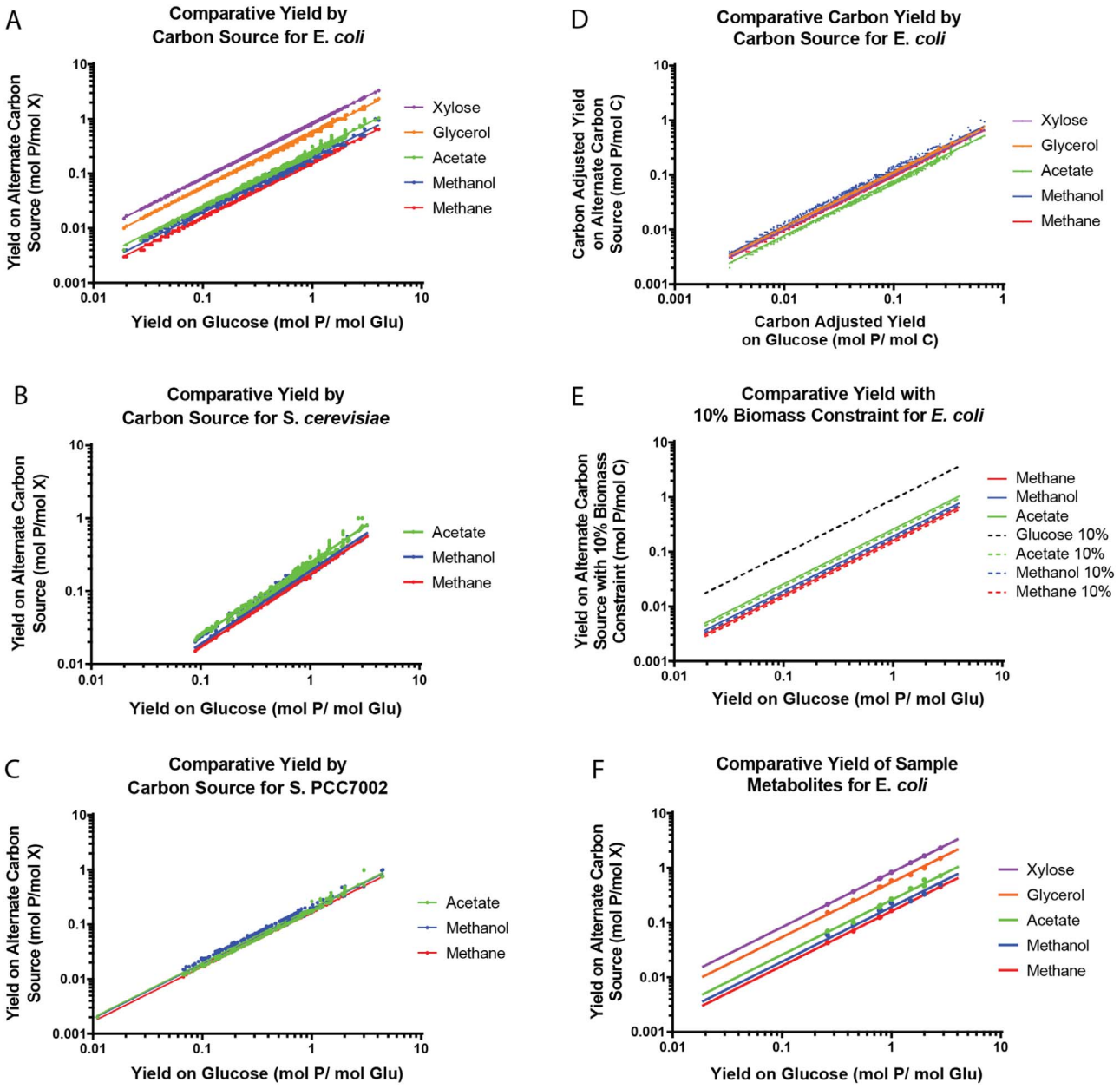

Fig. 2. The comparative product yields for alternative carbon sources compared to glucose are shown with individual products (points) as well as the least squares linear fit through the origin (lines). Equations for each alternative carbon source can be found in Supplemental Table 7. **A, B, and C:** Comparative yields for *E. coli*, *S. cerevisiae*, and *S.* PCC7002 respectively are shown for acetate, methanol, and methane carbon sources (*E. coli* also shows results for glycerol and xylose). **D:** *E. coli* comparative yields normalized on a per carbon basis on multiple substrates. **E:** *E. coli* comparative yields with a minimum of 10% of the maximum biomass growth rate (dashed lines) compared to no biomass requirement (solid lines). **F:** Comparative yields for a subset of data points from A as well as three heterologous pathway target products, as listed in Table 1, in comparison to the linear regressions determined in A.

Fig. 2**e**, a 10% biomass generation constraint resulted in ratios of theoretical yield that were approximately 10% lower. This finding shows that the consistent ratios of theoretical yield are not an artifact of running FBA without biomass production.

We included a set of heterologous pathways to test whether our predictions extended to non-native metabolites. This includes engineered pathways for production of butanol, isobutanol, and 3-methylbutanol. Each pathway branches from a different area of metabolism, specifically: acetyl-CoA, pyruvate, and branch-chain amino acid biosynthesis. Each pathway was run individually for each organism and tabulated along with a set of other metabolites of interest in Tables 1–3. Fig. 2**f** shows the results of this analysis in comparison to the linear regressions determined by the data in Fig. 2**a**. This test shows that important metabolic nodes and heterologous products both conform to the determined yield ratios.

We can analyze the relative importance of the different formaldehyde assimilation pathways by testing the effect of using only a single pathway at a time (Fig. 3**a–c**). When reduced to a single formaldehyde assimilation pathway from all three pathways simultaneously, the maximum theoretical yield of certain products decreased. For all three organisms growing on glucose, the formaldehyde assimilation pathways had little impact on the relative product yield. For *E. coli*, the DHA and RuMP pathways appear to act identically and with equal importance for production on methane and methanol. In *S. cerevisiae*, the RuMP pathway is the most effective formaldehyde assimilation pathway. In S. PCC 7002, all three pathways seem to have a similar effect whether acting alone or together in the full model. Including any formaldehyde assimilation pathway showed an increase in yield over the base model. These results do not include kinetic information, but do provide insight into which formaldehyde assimilation

Table 1
Model results for a set of interesting metabolites, including the products of the heterologous pathways that were tested (marked with *), for *E. coli*. These values are used to produce Fig. 2**f**.

	E. coli					
	Glucose	Xylose	Glycerol	Acetate	Methanol	Methane
Glycine	2.804	2.326	1.5	0.72	0.5	0.456
Leucine	0.778	0.639	0.439	0.202	0.167	0.126
Lysine	0.776	0.638	0.448	0.191	0.167	0.125
Serine	2	1.667	1	0.472	0.333	0.333
Tryptophan	0.449	0.371	0.255	0.101	0.091	0.07
Pyruvate	2	1.667	1	0.607	0.333	0.333
Succinate	1.5	1.25	0.75	0.423	0.25	0.25
Hexadecanoate	0.261	0.217	0.152	0.07	0.059	0.043
Butanol*	1	0.833	0.583	0.271	0.229	0.167
3-methylbutanol*	0.796	0.654	0.449	0.208	0.174	0.127
Isobutanol*	1	0.833	0.583	0.269	0.229	0.167

Table 2
Model results for a set of interesting metabolites, including the products of the heterologous pathways that were tested (marked with *), for *S. cerevisiae*. These values are used to produce Fig. 2**f**.

	S. cerevisiae			
	Glucose	Acetate	Methanol	Methane
Glycine	3	0.784	0.5	0.5
Leucine	0.753	0.175	0.163	0.132
Lysine	0.708	0.179	0.165	0.127
Serine	2	0.43	0.333	0.333
Tryptophan	0.426	0.087	0.091	0.073
Pyruvate	2	0.5	0.333	0.333
Succinate	1.5	0.386	0.25	0.25
Hexadecanoate	0.212	0.055	0.052	0.037
Butanol*	1	0.264	0.237	0.167
3-methylbutanol*	0.776	0.178	0.163	0.132
Isobutanol*	1	0.224	0.214	0.167

Table 3
Model results for a set of interesting metabolites, including the products of the heterologous pathways that were tested (marked with *), for *S.* PCC7002. These values are used to produce Fig. 2**f**. The PCC7002 model does not contain hexadecanoate.

	S. PCC7002			
	Glucose	Acetate	Methanol	Methane
Glycine	0.79	0.134	0.176	0.134
Leucine	0.508	0.086	0.114	0.086
Lysine	0.099	0.019	0.024	0.017
Serine	0.752	0.128	0.168	0.128
Tryptophan	0.26	0.044	0.058	0.044
Pyruvate	2	0.405	0.333	0.333
Succinate	1.474	0.32	0.25	0.25
Hexadecanoate	N/A	N/A	N/A	N/A
Butanol*	1	0.286	0.243	0.167
3-methylbutanol*	0.8	0.158	0.184	0.133
Isobutanol*	1	0.182	0.238	0.167

pathway should be included when engineering an organism for C_1 catabolism. Generally, the serine pathway is a poor choice based on stoichiometry when utilizing C_1 carbon sources.

Finally, we also considered inclusion of other efficient carbon utilization pathways to investigate their impact on maximum theoretical yield (non-oxidative glycolysis, Wood-Ljungdhal pathway, and 3-hydroxypropionate 4-hydroxybutyrate). None of the additional pathways showed a major increase in theoretical yield when compared with the same carbon source feed (glucose, methane, or methanol) (Fig. 3**d**). Specifically, the MCC functions for C_1 assimilation, but we were unable to show any improvement upon using the non-oxidative glycolysis pathway over the Embden-Meyerhof-Parnas pathway (Fig. 3**d**). (Bogorad et al., 2014)

3.3. Price adjusted yield ratio surfaces

Molar yields indicate that glucose is the preferred feedstock for biological chemical production, but on a per carbon basis, other feedstocks are more efficient. To evaluate the relative costs of different feedstocks, we created relative cost surfaces using estimated ranges of feedstock prices and the ratios of theoretical yield calculated from FBA. We used bulk purchase pricing and stock market values (specifically, natural gas and sugar prices) over a 5-year period to determine each carbon source's range of bulk purchase prices. We estimate that sugar prices are currently between $0.10 and $0.30/lb ($0.0264/mol to $0.0792/mol), methanol prices are between $1.00–1.60/gal ($0.01068/mol to $0.01709/mol), and methane prices are between $2.75-$4.50/MMBTU ($0.0022/mol to $0.0036/mol). It was more difficult to determine an estimate for acetate prices. Acetate comes in multiple forms and could be made commercially via a Bio-GTL process, which has not been economically analyzed in the public literature. Using bulk pricing for both sodium acetate and acetic acid, we calculated the highest price that we used (approximately $0.50/kg, or $0.03/mol). Acetate production from syngas in Bio-GTL processes could have very high yield (Hu et al., 2016) and therefore be less expensive. Therefore, we used a high molar conversion of syngas to acetate with a low cost of syngas to represent the lower bound on price ($0.05/kg, or $0.003/mol). This range is a best estimate and more information could adjust this range further.

Relative cost surfaces were constructed by plotting the relative feedstock cost of metabolites in an organism's genome-scale model (Fig. 4). The sliding color scheme represents the regions where the alternative carbon source is more expensive than glucose (red) for producing the average chemical, less expensive than glucose (blue), or equivalent (yellow). The surfaces showed little variation between three organisms studied, with glucose having a slightly bigger economic advantage in yeast. The surfaces show that methane is the only feedstock that is consistently less expensive than glucose at current feedstock prices. Conversely, methanol is more expensive than glucose as a feedstock over the range of current prices. The large uncertainty in acetate prices prevents a general statement, but low acetate prices have the potential to be a less expensive feedstock than glucose, albeit still more expensive than methane.

3.4. Discussion

Our analysis, based on feedstock price and theoretical conversion yields, suggests that methane is the most attractive feedstock for microbial cell factories. This assumes that technical barriers to using methane can be overcome. For instance, biological assimilation kinetics of methane tend to be relatively slow and are a rate-limiting step in methane conversion to value-added chemicals. The main cause of the slow kinetics is the long turnover time of the methane monooxygenase active site (Hwang et al., 2014). The reactivation of the active site is a slow process that results in an overall low methane assimilation rate. With protein engineering, it could be possible to overcome this barrier. There are also difficulties in scaling-up microbial production using a methane feedstock. Methane assimilation pathways require both methane and oxygen supply for effective function. This combination of gases can be explosive, which introduces a safety concern when using industrial-size reactors. Another difficulty is the slow mass transfer of methane into aqueous solutions (Conrado and Gonzalez, 2014). If these barriers are overcome, methane has the potential to be a more profitable feedstock than glucose.

A caveat to this analysis is that it only considers feedstock costs and does not consider differences in other costs associated with these feedstocks, such as operating costs, capital costs, conversion

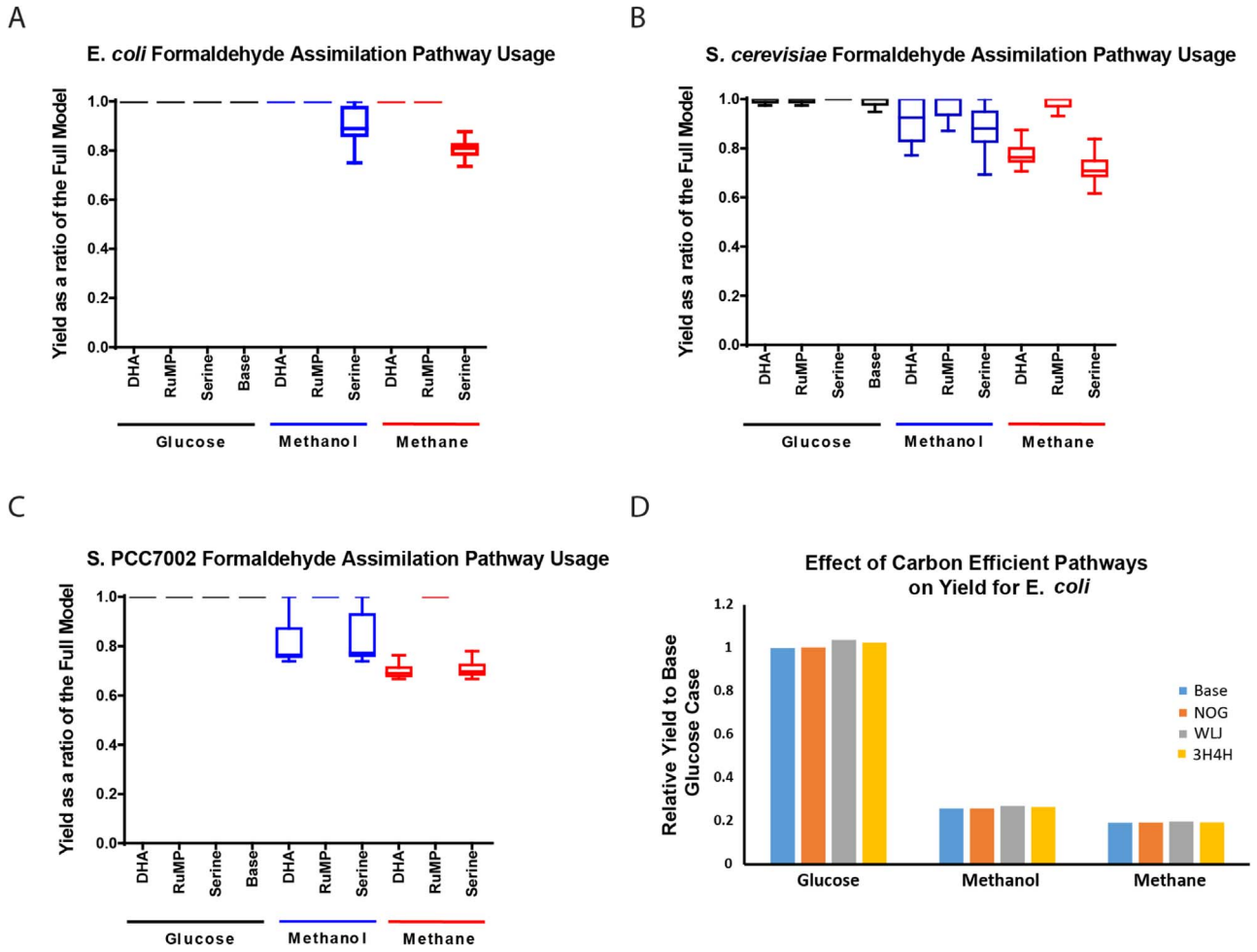

Fig. 3. A–C: C_1 assimilation pathway usage across different substrates and organisms. These box plots summarize the yield of each metabolite from the model and carbon source listed as a ratio to the yield from the full model using all three formaldehyde assimilation pathways. The base model has no formaldehyde assimilation pathways. The box plot whiskers are determined using Tukey method and outliers are not shown (outliers shown in Supplemental Figure 1). **D:** A comparison of different pathways for carbon efficient assimilation of glycolytic substrates in *E. coli*. All pathways provided similar yield ratios (using linear regression) and were tested only feeding the substrate listed below each set of bars. (Base = Oxidative Glycolysis only, NOG = Non-oxidative Glycolysis, WLI = Wood-Ljungdhal Pathway, 3HP4HB = 3-hydroxypropionate 4-hydroxybutyrate Pathway).

inefficiencies (i.e. operating at a fraction of theoretical yield), separations, wastes, etc. A true measure of profitability will require a more detailed technoeconomic analysis of any potential process. For instance, if a technological advance in methane-to-methanol catalytic conversion occurs, the price of methanol could drop considerably and make methanol more competitive with glucose. Methanol provides other technical advantages over methane such as faster mass transfer, faster uptake rate, simplified gassing, and reduced safety concerns that our feedstock analysis does not consider. However, considering current prices, it is clear that methane is the preferred feedstock.

If we are unable to engineer microbes for efficient methane assimilation for chemical production (i.e. achieve yields approaching theoretical limits), the more attractive strategy would be to convert methane to acetate (via syngas) instead of converting methane to methanol. The price of acetate is a large uncertainty in our analysis, but new BIO-GTL technologies that leverage less-expensive, nitrogen-containing syngas could make the lower end of our estimate range a reality. Assuming a low-cost bio-GTL process works at industrial scale, then acetate would compete with glucose as a feedstock.

Our analysis shows a consistent trend when comparing theoretical yields on different feedstocks, suggesting that a general relationship is derivable. This trend is interesting because it suggests that product yield varies with carbon source identity independent of the specific product (i.e. products have similar relative yields on different carbon sources). We postulate that this linear relationship is obtained because of the structure of metabolism in which catabolic and anabolic pathways are linked by common central metabolites. In other words, all of the substrates we simulated connect to central metabolism through the catabolic pathways described in the introduction, in the process generating NAD(P)H and ATP to varying extents depending on the substrate. Conversely, all products (except those metabolites found in the catabolic pathways) are produced from the same anabolic pathways independent of carbon source. Therefore the difference in a product's yield on different carbon sources can be traced to the difference in NAD(P)H/ATP produced via the catabolic pathways used to convert carbon sources into precursors for that product.

Thermodynamics could provide a possible explanation for the linear relationship between product yields on different feedstocks. A thermodynamic estimate of the maximum theoretical product yield from a specific substrate can be calculated using the carbon number and degree of reduction of both the substrate and product (Doran, 2012). This is calculated using Eq. (3), where f_{max} is the number of moles of product that can be made from 1 mol of substrate, w and j are the number of carbon atoms in the substrate and product and γ_s and γ_p are the degree of reduction of substrate and product, respectively (Doran, 2012).

$$f_{max} = \frac{w\gamma_s}{j\gamma_p} \tag{3}$$

For a given product, j and γ_p will remain constant when comparing different substrates, while w and γ_s will be unique to the substrate used.

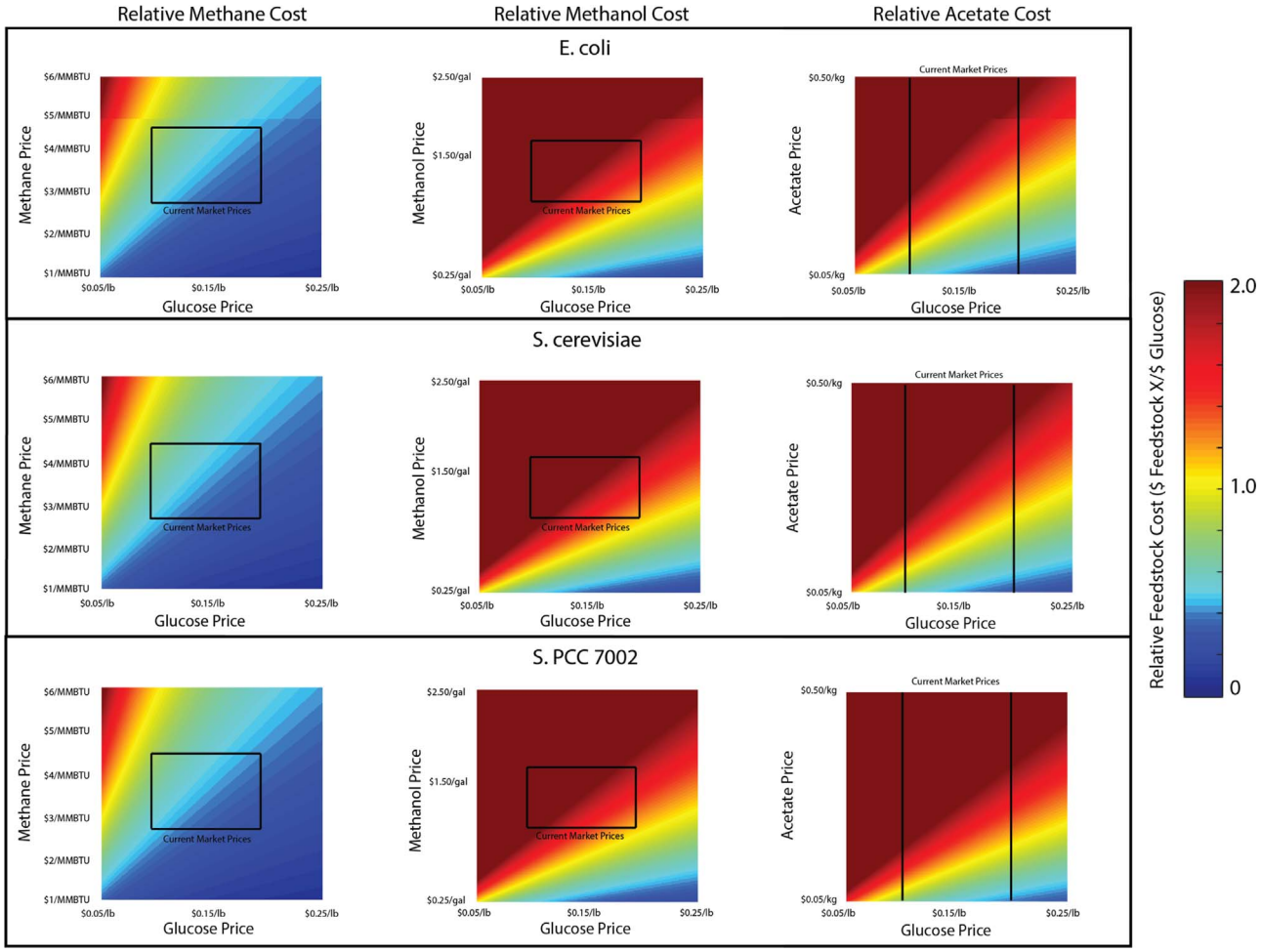

Fig. 4. Surfaces of price adjusted yield ratios calculated over a range of methane, methanol, and glucose substrate prices. The black box represents the range of current market prices (we did not estimate market prices for acetate price). Values above one indicate higher alternate carbon source profitability, while values below one indicate higher glucose profitability.

This allows for a comparison between maximum theoretical yields of different substrates on a thermodynamic basis. The numerator of Eq. (3) is 8 for methane, 6 for methanol, 8 for acetate, and 24 for glucose. This implies yields from glucose will be 3 times higher than from methane or acetate and 4 times higher than yields from methanol. When normalized for carbon content, methane generates a theoretical yield twice that of glucose. In our analysis, when yields were normalized to the carbon number in the feedstock, the largest difference between feedstocks was significantly less than 2 (Fig. 2). Therefore, the degree of reduction is not completely responsible for remaining difference in yields on various feedstocks. One reason for the discrepancy is the requirement of additional electrons and energy in the specific biological pathways (e.g. MMO) used to conduct the transformations. For this reason, analysis using genome-scale metabolic models is an improvement over analysis using just stoichiometry.

Acknowledgements

This work was supported by a grant from the US National Science Foundation (CBET-1149678) and the US Department of Energy (DE-SC0008103). ADC is the recipient of a NSF Graduate Research Fellowship (DGE-1256259) and a NIH Biotechnology Training Program Fellowship (NIGMS - 5 T32 GM08349).

Appendix A. Supporting information

Supplementary data associated with this article can be found in the online version at http://dx.doi.org/10.1016/j.meteno.2017.07.002.

References

Begemann, M.B., Zess, E.K., Walters, E.M., Schmitt, E.F., Markley, A.L., Pfleger, B.F., 2013. An organic acid based counter selection system for cyanobacteria. PLoS One 8, e76594. http://dx.doi.org/10.1371/journal.pone.0076594.

Bogorad, I.W., Chen, C., Theisen, M.K., Wu, T., Schlenz, A.R., Lam, A.T., 2014. Building carbon – carbon bonds using a biocatalytic methanol condensation cycle. doi: ⟨http://dx.doi.org/10.1073/pnas.1413470111⟩.

Bogorad, I.W., Lin, T.-S., Liao, J.C., 2013. Synthetic non-oxidative glycolysis enables complete carbon conservation. Nature 502, 693–697. http://dx.doi.org/10.1038/nature12575.

Conrado, R.J., Gonzalez, R., 2014. Envisioning the bioconversion of methane to liquid fuels. Science 343, 621–623. http://dx.doi.org/10.1126/science.1246929.

Doran, P.M., 2012. Bioprocess Engineering Principles, 2nd ed. Academic Presshttp://dx.doi.org/10.1016/S0892-6875(96)90075-8.

Haynes, C. a., Gonzalez, R., 2014. Rethinking biological activation of methane and conversion to liquid fuels. Nat. Chem. Biol. 10, 331–339. http://dx.doi.org/10.1038/nchembio.1509.

Howarth, R.W., Ingraffea, A., Engelder, T., 2011. Natural gas: should fracking stop? Nature 477, 271–275. http://dx.doi.org/10.1038/477271a.

Hu, P., Chakraborty, S., Kumar, A., Woolston, B.M., Liu, H., Emerson, D., Stephanopoulos, G., 2016. Integrated bioprocess for conversion of gaseous substrates to liquids. Proc. Natl. Acad. Sci.

Hwang, I.Y., Lee, S.H., Choi, Y.S., Park, S.J., Na, J.G., Chang, I.S., Kim, C., Kim, H.C., Kim, Y.H., Lee, J.W., Lee, E.Y., 2014. Biocatalytic conversion of methane to methanol as a key step for development of methane-based biorefineries. J. Microbiol. Biotechnol. 24, 1597–1605.

Klein-Marcuschamer, D., Simmons, B.A., Blanch, H.W., 2011. Techno-economic analysis of a lignocellulosic ethanol biorefinery with ionic liquid pre-treatment. Biofuels, Bioprod. Bioref. 5, 562–569. http://dx.doi.org/10.1002/bbb.303.

McEwen, J.T., Machado, I.M.P., Connor, M.R., Atsumi, S., 2013. Engineering synechococcus elongatus PCC 7942 for continuous growth under diurnal conditions. Appl. Environ. Microbiol. 79, 1668–1675. http://dx.doi.org/10.1128/AEM.03326-12.

Mo, M.L., Palsson, B.O., Herrgård, M.J., 2009. Connecting extracellular metabolomic measurements to intracellular flux states in yeast. BMC Syst. Biol. 3, 37. http://dx.

doi.org/10.1186/1752-0509-3-37.
Müller, J.E.N., Meyer, F., Litsanov, B., Kiefer, P., Potthoff, E., Heux, S., Quax, W.J., Wendisch, V.F., Brautaset, T., Portais, J.-C., Vorholt, J.A., 2015. Engineering Escherichia coli for methanol conversion. Metab. Eng. 28, 190–201. http://dx.doi.org/10.1016/j.ymben.2014.12.008.
Orth, J.D., Conrad, T.M., Na, J., Lerman, J.A., Nam, H., Feist, A.M., Palsson, B.Ø., 2011. A comprehensive genome-scale reconstruction of Escherichia coli metabolism–2011. Mol. Syst. Biol. 7, 535. http://dx.doi.org/10.1038/msb.2011.65.
Orth, J.D., Thiele, I., Palsson, B.O., 2010. What is flux balance analysis? Nat. Biotechnol. 28, 245–248. http://dx.doi.org/10.1038/nbt.1614.
Papoutsakis, E.T., 2000. Equations and calculations for fermentations of butyric acid bacteria. Biotechnol. Bioeng. 67, 813–826. http://dx.doi.org/10.1002/(SICI)1097-0290(20000320)67:6<813::AID-BIT17>3.0.CO;2-X.
Salmon, R., Logan, A., 2013. Flaring Up: North Dakota Natural Gas Flaring More Than Doubles in Two Years.
Vu, T.T., Hill, E.A., Kucek, L.A., Konopka, A.E., Beliaev, A.S., Reed, J.L., 2013. Computational evaluation of Synechococcus sp. PCC 7002 metabolism for chemical production. Biotechnol. J. 8, 619–630. http://dx.doi.org/10.1002/biot.201200315.
Whitaker, W.B., Sandoval, N.R., Bennett, R.K., Fast, A.G., Papoutsakis, E.T., 2015. Synthetic methylotrophy: engineering the production of biofuels and chemicals based on the biology of aerobic methanol utilization. Curr. Opin. Biotechnol. 33, 165–175. http://dx.doi.org/10.1016/j.copbio.2015.01.007.
Yurimoto, H., Kato, N., Sakai, Y., 2005. Assimilation, dissimilation, and detoxification of formaldehyde, a central metabolic intermediate of methylotrophic metabolism. Chem. Rec. 5, 367–375. http://dx.doi.org/10.1002/tcr.20056.